Available online at www.sciencedirect.com
SCIENCE DIRECT
Tetrahedron Letters
Tetrahedron Letters 47 (2006) 2887–2891

Synthesis, structure, and both cathodic and anodic reversible redox reactions of benzochalcogenophenes containing ferrocene units

Satoshi Ogawa,* Kenji Kikuta, Hiroki Muraoka, Fumihito Saito and Ryu Sato*

Department of Chemical Engineering, Faculty of Engineering, Iwate University, Morioka 020-8551, Japan

Received 2 February 2006; revised 17 February 2006; accepted 21 February 2006
Available online 9 March 2006

Abstract—2,3-Diferrocenylbenzo[*b*]thiophene and 1,3-diferrocenylbenzo[*c*]thiophene have been systematically and selectively synthesized from benzo[*b*]thiophene and phthaloyl dichloride, respectively. Characterization of the molecules was performed by physical and spectroscopic means and X-ray crystallographic analyses. The cyclic voltammograms of the novel thiophene derivatives containing ferrocene fragments showed a well-defined reversible cathodic step derived from the unusually stable thiophene radical anions and two distinct reversible anodic steps derived from ferrocenium cations separated from each other by a thiophene heterocycle. 1,3-Diferrocenylbenzo[*c*]selenophene was also synthesized in a similar manner for formation of 1,3-diferrocenylbenzo[*c*]thiophene by the use of bis(dimethylaluminum) selenide as a selenating reagent.
© 2006 Elsevier Ltd. All rights reserved.

In recent years, molecules comprising multiple reduction–oxidation (redox) centers have been attracting attention in the field of material science due to the potentiality of new organic semi-conducting materials with application.[1] Moreover, this kind of molecule having more than two redox-active metal centers is a fundamentally attractive target for the study of multi-electron transfer processes via the mixed valence state derived from these multi-metallic systems.[2] On the other hand, interest in the design of novel redox-active organic centers by the use of a 7π electron framework[3] containing group 16 elements has led us to explore the synthesis of new five-membered heterocycles containing sulfur and/or selenium atom(s). This time our studies are aimed at the design of reversible multi-steps redox systems using simple molecules with both organic and organometallic electron transfer fragments. Although the synthesis and characterization of substituted benzochalcogenophenes have been reported,[4] there is no report concerning benzannulated thiophene and selenophene containing a ferrocene fragment on the five-membered heterocyclic unit, which are of structural and redox characteristic interest, in contrast to benzannulated chalcogenophene, namely, 1,3-dithienylbenzo[*c*]thiophene and -selenophene.[5] Recently, we reported a new type of multi-steps reversible redox systems using organic–organometallic hybrid molecules, 1-ferrocenyl- and 1,9-diferrocenyl-thianthrenes.[6] Therefore, we have designed 2,3-diferrocenylbenzo[*b*]thiophene, 1,3-diferrocenylbenzo[*c*]chalcogenophenes as both cathodic and anodic multiple-redox active organic–organometallic hybrid molecules. In this letter, we provide the details on the synthesis, structural characterization, and electrochemical properties of 2,3-diferrocenylbenzo[*b*]thiophene, 1,3-diferrocenylbenzo[*c*]thiophene, and 1,3-diferrocenylbenzo[*c*]selenophene.

The synthesis of 2,3-diferrocenylbenzo[*b*]thiophene (**1**) was achieved through the transition metal-catalyzed cross-coupling reaction[7] of 2,3-dibromobenzo[*b*]thiophene, which was prepared by general bromination with bromine,[8] with ferrocenylzinc chloride in the presence of a catalytic amount of bis(triphenylphophine)palladium(II) dichloride, $(PPh_3)_2PdCl_2$, in tetrahydrofuran (THF) under reflux condition (Scheme 1). On the other hand, we employed phthaloyl dichloride as a starting material for the synthesis of 1,3-diferrocenylbenzo[*c*]thiophene (**2**). However, two acid chlorides in the *ortho* position are too reactive toward nucleophilic substitution by the use of Grignard or organolithium reagents even

Keywords: Thiophene; Selenophene; Ferrocene; Cyclic voltammetry; Redox reaction.
* Corresponding authors. Tel./fax: +81 19 621 6934; e-mail: ogawa@iwate-u.ac.jp

0040-4039/$ - see front matter © 2006 Elsevier Ltd. All rights reserved.
doi:10.1016/j.tetlet.2006.02.122

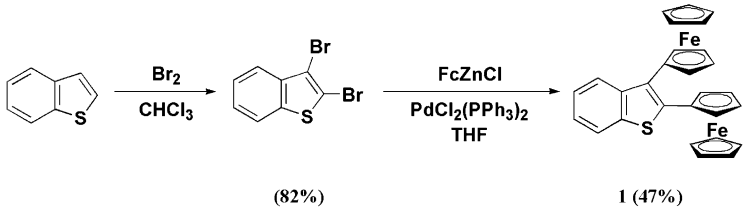

Scheme 1.

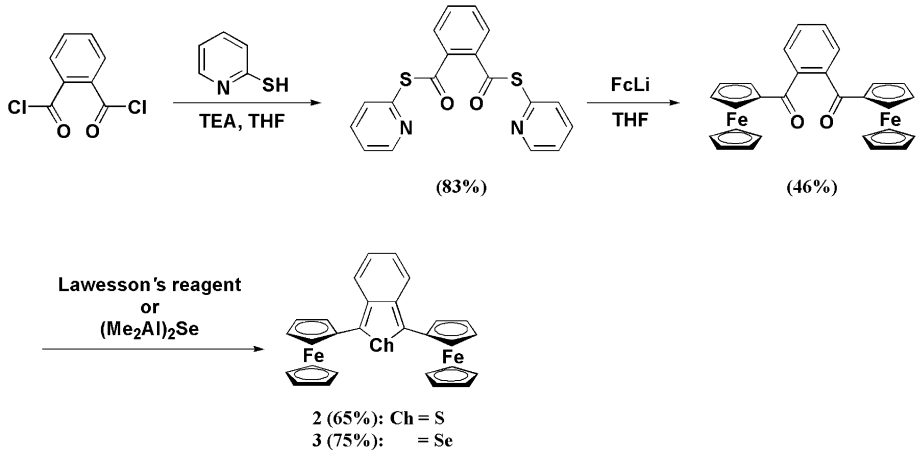

Scheme 2.

at low temperature. Therefore, we synthesized 1,2-di[*S*-(2-pyridinyl)]benzenedithioate which has two functional groups with lower reactivity as compared with phthaloyl dichloride by the modified method previously reported.[9] Since we obtained 1,2-di[*S*-(2-pyridinyl)]benzenedithioate, the next step consisted of performing the reaction with a ferrocenyllithium reagent. The ferrocenyllithium, which was prepared from ferrocene with *t*-butyllithium, was slowly added at −60 °C to 1,2-di[*S*-(2-pyridinyl)]benzenedithioate in a solution of THF. The mixture was stirred at −60 °C for 30 min and finally quenched by addition of 2 mol dm^{-3} HCl aqueous solution. After usual work-up, *ortho* diferrocenoylbenzene was obtained in moderate yield. Finally, the isothianaphthene core was formed through ring closure of *ortho* diferrocenoylbenzene by means of Lawesson's reagent to give 1,3-diferrocenylbenzo[*c*]thiophene (**2**) in moderate yield (Scheme 2). In the case of the synthesis of 1,3-diferrocenylbenzo[*c*]selenophene (**3**), the ring-closure reaction was performed by the use of bis(dimethylaluminum) selenide developed by Segi and Zingaro[10] as a selenating reagent.

Structural characterization of new benzothiophenes **1**, **2**, and benzoselenophene **3** was performed by physical and spectroscopic means.[11] In addition, single crystals of **1**–**3** were successfully obtained by slow crystallization from effectual organic solvents at room temperature. The crystal structures of **1**[12] (Fig. 1), **2**[13] (Fig. 2), and **3**[14] (Fig. 3) were determined by X-ray crystallographic analyses and revealed that two ferrocene fragments were located in anti-conformation, respectively, having the dihedral angles of 34.3(5) and 42.3(4)° for **1**, −23.7(2) and +30.0(2)° for **2**, −21.9(5) and +30.1(5)° for **3**. The C–C distances between the ferrocenyl carbon and the carbon(s) next to thienyl sulfur suggest a double bond character because the lengths of 1.458(4) Å for **1**, 1.461(2) and 1.461(2) Å for **2**, 1.451(6) and 1.447(5) Å

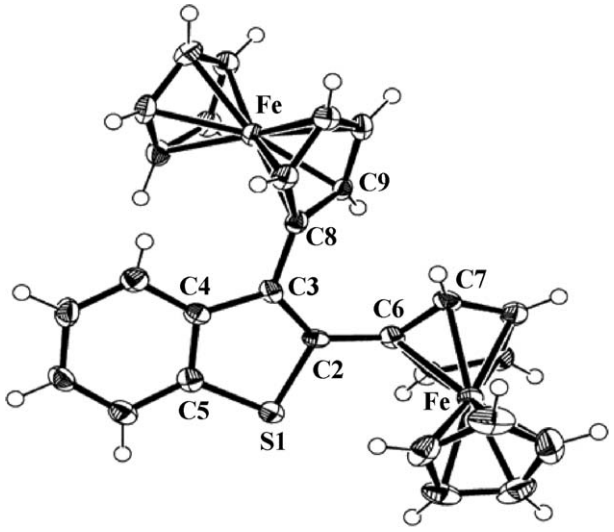

Figure 1. ORTEP drawing of compound **1**. Dichloromethane molecule is omitted for clarity. Thermal ellipsoids are drawn at 50% probability. Selected bond distances (Å), bond angles (°), and dihedral angles (°): S1–C2 1.760(4), C2–C3 1.355(4), C3–C4 1.451(5), C4–C5 1.404(5), C5–S1 1.735(3), C2–C6 1.458(4), C3–C8 1.490(5), S1–C2–C3 112.5(3), C2–C3–C4 113.0(3), C3–C4–C5 111.3(2), C4–C5–S1 112.2(2), C5–S1–C2 91.0(2), C8–C3–C2 122.3(3), C6–C2–C3 130.3(3), C7–C6–C2–C3 34.3(5), C2–C3–C8–C9 42.3(4), C6–C2–C3–C8 4.8(5).

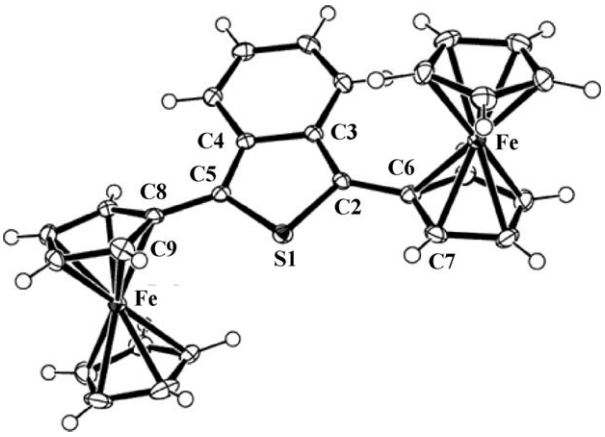

Figure 2. ORTEP drawing of compound **2**. Thermal ellipsoids are drawn at 50% probability. Selected bond distances (Å), bond angles (°), and dihedral angles (°): S1–C2 1.720(2), C2–C3 1.393(2), C3–C4 1.443(2), C4–C5 1.390(2), C5–S1 1.714(2), C2–C6 1.461(2), C5–C8 1.461(2), S1–C2–C3 110.2(1), C2–C3–C4 112.4(2), C3–C4–C5 112.9(1), C4–C5–S1 110.3(1), C5–S1–C2 94.16(8), S1–C2–C6–C7 −23.7(2), C9–C8–C5–S1 30.0(2).

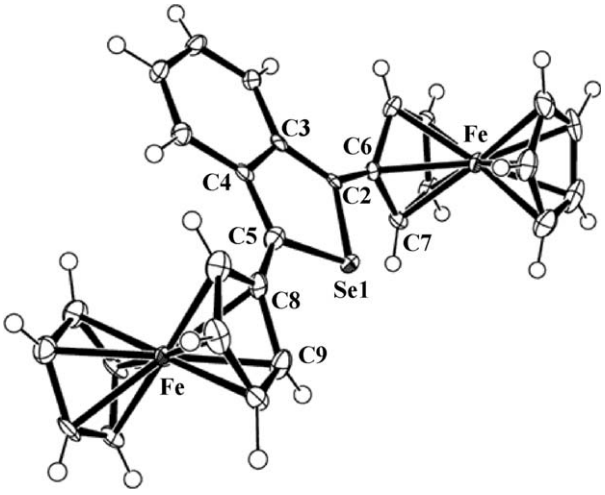

Figure 3. ORTEP drawing of compound **3**. Thermal ellipsoids are drawn at 50% probability. Selected bond distances (Å), bond angles (°), and dihedral angles (°): Se1–C2 1.867(4), C2–C3 1.381(5), C3–C4 1.456(5), C4–C5 1.386(5), C5–Se1 1.862(4), C2–C6 1.447(5), C5–C8 1.451(6), C5–Se1–C2 89.8(4), Se1–C2–C3 109.9(3), C2–C3–C4 115.3(3), C3–C4–C5 115.0(3), C4–C5–Se1 110.0(3), C9–C8–C5–Se1 −21.9(5), Se1–C2–C6–C7 30.1(5).

for **3** are significantly shorter than that of the sp^2–sp^2 single bond (1.516 Å).[15]

The redox properties of chalcogenophene–ferrocene systems have been furnished by electrochemical measurements; the data are collected in Table 1 and cyclic voltammograms (CV) of compounds **1**–**3** are shown in Figure 4. The dominant feature of CV scans of **1**–**3** at concentrations 2.0 mmol dm^{-3} in THF/0.1 mol dm^{-3} $^{n}Bu_4NPF_6$ is three one-electron redox couples, $E_{1/2} =$ −2.87, +0.22, +0.41 V for **1**; −2.38, +0.14, +0.34 V for **2**; −2.31, +0.15, +0.39 V for **3**; versus Ag/Ag^{+}, respectively, that is well-defined reversibility. At negative scan, the reduction of **1**–**3** is electrochemically reversible and a cathodic product wave appears, assigned to formation of the corresponding radical anion. On the other hand, at positive scan, the oxidation of **1**–**3** is also electrochemically reversible and two anodic product waves appear, assigned to stepwise formation of the corresponding mono- and bis-(ferrocenium cation).

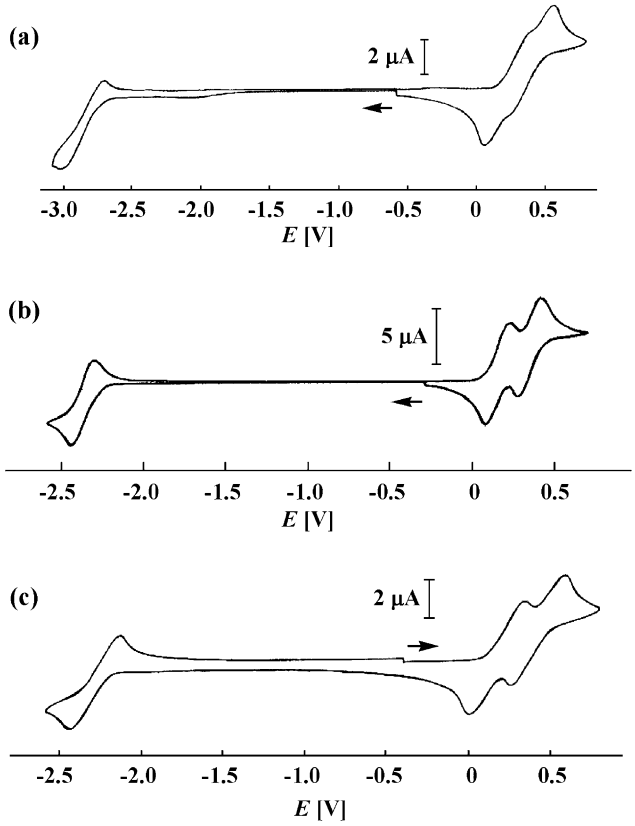

Figure 4. Cyclic voltammograms of **1** (a), **2** (b), and **3** (c).

Table 1. Redox potentials (V vs Ag/Ag^{+})[a] of diferrocenylbenzochalcogenophene **1**, **2**, and **3**

	1			2			3		
	First	Second	Third	First	Second	Third	First	Second	Third
E_{pa}	−2.71	+0.38	+0.56	−2.31	+0.21	+0.41	−2.19	+0.27	+0.51
E_{pc}	−3.02	+0.06	+0.25	−2.45	+0.07	+0.27	−2.42	+0.02	+0.26
$E_{1/2}$	−2.87	+0.22	+0.41	−2.38	+0.14	+0.34	−2.31	+0.15	+0.39

[a] Conditions: concentration, 2 mmol dm^{-3} sample in 0.1 mol dm^{-3} $[Bu_4N]^{+}[PF_6]^{-}$/THF solution; temperature, 223 K for **1**, 293 K for **2**, 233 K for **3**; working electrode, glassy-carbon; reference electrode, Ag/0.01 mol dm^{-3} $AgNO_3$ in 0.1 mol dm^{-3} $[Bu_4N]^{+}[PF_6]^{-}/CH_3CN$ solution; counter electrode, Pt; scan rate, 200 mV s^{-1} for **1**, and 100 mV s^{-1} for **2** and **3**.

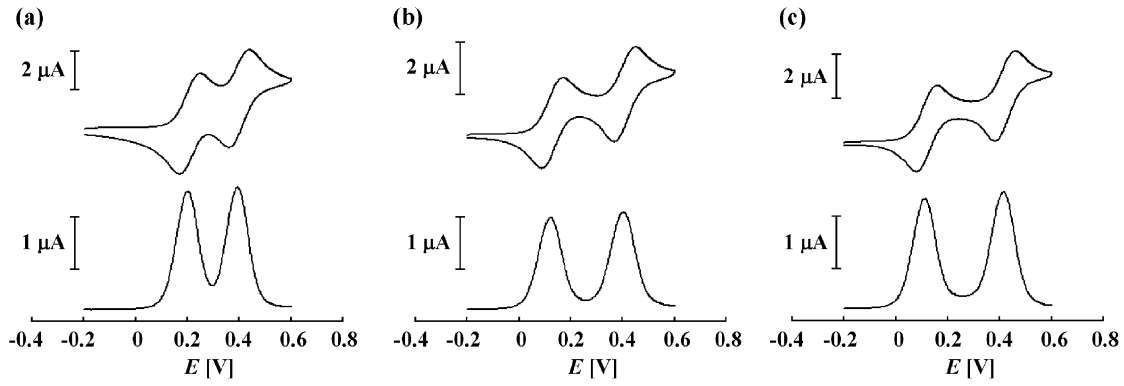

Figure 5. Cyclic (top) and differential pulse (bottom) voltammograms of **1** (a), **2** (b), and **3** (c).

By CV and differential pulse voltammograms (DPV) measurements of **1**–**3** employing dichloromethane (CH_2Cl_2) as a solvent, the oxidation waves derived from the ferrocene fragments showed good separated and well-defined reversible one-electron redox couples (Fig. 5).[2a] The differences between the first and second half-potentials ($\Delta E_{1/2} = E^1_{1/2} - E^2_{1/2}$) for the Fe(II)–Fe(III) and Fe(III)–Fe(III) couples of **1**, **2**, and **3** were 192, 280, and 305 mV, respectively (Table 2). These results suggest that the structural difference between diferrocenylbenzothiophenes **1** and **2** based on the annulation mode and the substituent position should cause the differences in their redox behavior and thermodynamic stability in mixed-valence intermediates. The comproportionation constants (K_c)[2a] for the Fe(II)–Fe(III) mixed-valence state estimated from $\Delta E_{1/2}$ were 1.1×10^5 for **2** and 3.0×10^5 for **3**. Therefore, the electronic interaction between the metal center of ferrocene and the ferrocenium cation in the mixed-valence state of **2** and **3** can be expected to be strong because of potential through-bond and/or through-space interactions. In the case of compound **1**, it is difficult to discuss the comproportionation constant K_c, because it has essentially different oxidation potentials based on the position of ferrocenes.

In conclusion, we have synthesized and characterized novel benzochalcogenophenes containing ferrocene units. The electrochemical properties showed reversible multi-electron transfer phenomena assigned to chalcogenophene (organic) and ferrocene (organometallic) fragments owing to good stability of the negative-charged reduction products (radical anions) and positive-charged oxidation products (mono- and bis-ferrocenium cations). Therefore, we succeeded in establishing a new type of multi-steps reversible redox systems using neutral organic–organometallic hybrid molecules.

Table 2. Redox potentials (V vs Ag/Ag^+)[a] of **1**, **2**, and **3**

	$E^1_{1/2}$ (V)	$E^2_{1/2}$ (V)	$\Delta E_{1/2}$[b] (mV)
1	+0.21	+0.40	+192
2	+0.13	+0.41	+280
3	+0.12	+0.42	+305

[a] Conditions: concentration, 1 mmol dm^{-3} sample in 0.1 mol dm^{-3} $[Bu_4N]^+[PF_6]^-/CH_2Cl_2$ solution; temperature, 281 K; working electrode, glassy-carbon; reference electrode, Ag/0.01 mol dm^{-3} $AgNO_3$ in 0.1 mol dm^{-3} $[Bu_4N]^+[PF_6]^-/CH_3CN$ solution; counter electrode, Pt; scan rate, 100 mV s^{-1}.

[b] $\Delta E_{1/2} = E^2_{1/2} - E^1_{1/2}$.

Acknowledgements

This work was supported by Grant-in-Aid for Scientific Research (No. 15550023) from the Ministry of Education, Culture, Sports, Science, and Technology. We thank Ms. Shiduko Nakajo (Division of Elemental Analysis, Iwate University), for elemental analyses.

References and notes

1. Fichou, D. *Handbook of Oligo- and Polythiophenes*; VCH: Weinheim, 1999; Naguyen, P.; Gómez-Elipe, P.; Manners, I. *Chem. Rev.* **1999**, *99*, 1515–1548; Iyoda, M.; Hasegawa, M.; Miyake, Y. *Chem. Rev.* **2004**, *104*, 5058–5113.
2. (a) Barlow, S.; O'Hare, D. *Chem. Rev.* **1997**, *97*, 637–669; Dong, T.-Y.; Lee, W.-Y.; Su, P.-T.; Chang, L.-S.; Lin, K.-J. *Organometallics* **1998**, *17*, 3323–3330; Nishihara, H. *Bull. Chem. Soc. Jpn.* **2001**, *74*, 19–29; Ito, T.; Hamaguchi, T.; Nagino, H.; Yamaguchi, T.; Kido, H.; Zavarine, I. S.; Richmond, T.; Washington, J.; Kubiak, C. P. *J. Am. Chem. Soc.* **1999**, *121*, 4625–4632; Hamaguchi, T.; Nagano, H.; Hoki, K.; Kido, H.; Yamaguchi, T.; Breedlove, B. K.; Ito, T. *Bull. Chem. Soc. Jpn.* **2005**, *78*, 591–598.
3. Schröder, D.; Schwarz, H.; Löbrecht, B.; Koch, W.; Ogawa, S. *Eur. J. Inorg. Chem.* **1998**, 983–987; Ogawa, S.; Kikuchi, M.; Kawai, Y.; Niizuma, S.; Sato, R. *Chem. Commun.* **1999**, 1891–1892; Ogawa, S.; Ohmiya, T.; Kikuchi, T.; Kawaguchi, A.; Saito, S.; Sai, A.; Ohyama, N.; Kawai, Y.; Niizuma, S.; Nakajo, S.; Kimura, T.; Sato, R. *J. Organomet. Chem.* **2000**, *611*, 136–145; Nagahora, N.; Ogawa, S.; Yoshimura, S.; Kawai, Y.; Sato, R. *Bull. Chem. Soc. Jpn.* **2003**, *76*, 1043–1054.
4. Buckland, P. R.; Hacker, N. P.; McOmie, J. F. W. *J. Chem. Soc., Perkin Trans. 1* **1983**, 1443–1448; Nicolaides, D. N.; Litinas, K. E.; Argyropoulos, N. G. *J. Chem. Soc., Perkin Trans. 1* **1986**, 415–419; Brooke, G. M.; Mawson, S. D. *J. Chem. Soc., Perkin Trans. 1* **1990**, 1919–1923; Volz, W.; Voß, J. *Synthesis* **1990**, 670–674; Ishii, A.; Nakayama, J.; Kazami, J.; Ida, Y.; Nakamura, T.; Hoshino, M. *J. Org. Chem.* **1991**, *56*, 78–82; Okuda, Y.; Lakshmikantham, M. V.; Cava, M. P. *J. Org. Chem.* **1991**, *56*, 6024–6026; Selegue, J. P.; Swarat, K. A. *J. Am. Chem. Soc.* **1993**, *115*, 6448–6449; Roncali, J. *Chem. Rev.* **1997**,

97, 173–205; Müller, E.; Thomas, R.; Sauerbier, M.; Langer, E.; Streichfuss, D. *Tetrahedron Lett.* **1971**, *12*, 521–524; Saris, L.; Cava, M. *J. Am. Chem. Soc.* **1976**, *98*, 867–868; Cowan, D. O.; Kini, A.; Chiang, L. Y.; Lerstrup, K.; Talham, D. R.; Poehler, T. O.; Bloch, A. N. *Mol. Cryst. Liq. Cryst.* **1982**, *86*, 1–4.

5. Lorcy, D.; Cava, M. P. *Adv. Mater.* **1992**, *4*, 562–564; Bauerle, P.; Gotz, G.; Emerle, P.; Port, H. *Adv. Mater.* **1992**, *4*, 564–568; Musinanni, S.; Ferraris, J. P. *J. Chem. Soc., Chem. Commun.* **1993**, 172–174; Mohanakrishnan, A. K.; Amaladass, P. *Tetrahedron Lett.* **2005**, *46*, 4225–4229; Mohanakrishnan, A. K.; Amaladass, P. *Tetrahedron Lett.* **2005**, *46*, 7201–7204.
6. Ogawa, S.; Muraoka, H.; Sato R. *Tetrahedron Lett.* **2006**, *47*, 2479–2483.
7. Iyoda, M.; Kondo, T.; Okabe, T.; Matsuyama, H.; Sasaki, S.; Kuwatani, Y. *Chem. Lett.* **1997**, 35–36; Iyoda, M.; Okabe, T.; Katada, M.; Kuwatani, Y. *J. Organomet. Chem.* **1998**, *569*, 225–233; Iyoda, M.; Takano, T.; Otani, N.; Ugawa, K.; Yoshida, M.; Matsuyama, H.; Kuwatani, Y. *Chem. Lett.* **2001**, 1310–1311.
8. Heynderickx, A.; Samat, A.; Guglielmetti, R. *Synthesis* **2002**, *2*, 213–216.
9. Araki, M. *Bull. Chem. Soc. Jpn.* **1974**, *47*, 1777–1780; Kiebooms, R. H. L.; Adriaensens, P. J. A.; Vanderzande, D. J. M.; Gelan, J. M. J. V. *J. Org. Chem.* **1997**, *62*, 1473–1480.
10. Li, G. M.; Zingaro, R. A.; Segi, M.; Reibenspies, J. H.; Nakajima, T. *Organometallics* **1997**, *16*, 756–762.
11. Spectral and physical data for **1**: brown crystals; mp 175.9–176.3 °C; ^{1}H NMR (400 MHz, $CDCl_3$): δ 4.06 (s, 5H, free-Cp), 4.15 (s, 5H, free-Cp), 4.25 (t, $J = 1.9$ Hz, 2H, C_5H_4), 4.26 (t, $J = 1.9$ Hz, 2H, C_5H_4), 4.32 (t, $J = 1.9$ Hz, 2H, C_5H_4), 4.36 (t, $J = 1.9$ Hz, 2H, C_5H_4), 7.35 (td, $J = 1.3$, 8.0 Hz, 1H, ArH), 7.44 (td, $J = 1.3$, 8.0 Hz, 1H, ArH), 7.78 (d, $J = 8.0$ Hz, 1H, ArH), 8.57 (d, $J = 8.0$ Hz, 1H, ArH); ^{13}C NMR (101 MHz, $CDCl_3$): δ 68.3, 68.1, 69.2, 69.6, 70.0, 70.6, 80.5, 80.8, 121.7, 123.5, 123.8, 124.1, 128.9, 138.7, 138.9, 140.0; IR (KBr) ν 3100, 2362, 1412, 1320, 1107, 1000, 820, 733, 490 cm^{-1}; MS (70 eV) m/z 502 (M^+). Anal. Calcd for $C_{28}H_{22}Fe_2S$: C, 66.96; H, 4.42. Found: C, 67.28; H, 4.65. Spectral and physical data for **2**: purple crystals; mp 196.0 °C (decomp.); ^{1}H NMR (400 MHz, $CDCl_3$): δ 4.18 (s, 10H, free-Cp), 4.39 (t, $J = 1.8$ Hz, 4H, C_5H_4), 4.74 (t, $J = 1.8$ Hz, 4H, C_5H_4), 7.00 (dd, $J = 3.1$, 6.9 Hz, 2H, ArH), 7.81 (dd, $J = 3.1$, 6.9 Hz, 2H, ArH); ^{13}C NMR (101 MHz, $CDCl_3$): δ 68.4, 68.6, 69.9, 80.2, 121.9, 123.0, 130.7, 135.2; IR (KBr) ν 3093, 2927, 1741, 1644, 1464, 804, 740 cm^{-1}; MS (70 eV) m/z 502 (M^+). Anal. Calcd for $C_{28}H_{22}Fe_2S$: C, 66.96, H, 4.42. Found: C, 66.80, H, 4.47. Spectral and physical data for **3**: purple crystals; mp 196.0 °C (decomp.); ^{1}H NMR (400 MHz, $CDCl_3$): δ 4.19 (s, 10H, free-Cp), 4.39 (t, $J = 1.8$ Hz, 4H, ArH), 4.69 (t, $J = 1.8$ Hz, 4H, ArH), 6.86 (dd, $J = 3.1$, 7.1 Hz, 2H, ArH), 7.67 (dd, $J = 3.1$, 7.1 Hz, 2H, ArH); ^{13}C NMR (101 MHz, $CDCl_3$): δ 68.7, 69.2, 70.2, 82.4, 122.5, 122.7, 137.6, 139.6; ^{77}Se NMR (76 MHz, $CDCl_3$): δ 687.8; IR (KBr) ν 3090, 2346, 1655, 1410, 1314, 1104, 1000, 838, 819, 741, 478 cm^{-1}; MS (70 eV) m/z 550 (M^+). Anal. Calcd for $C_{28}H_{22}Fe_2Se$: C, 61.24; H, 4.04. Found: C, 60.99, H, 4.34.
12. Crystal data for **1**·CH_2Cl_2: $M = 587.17$, $C_{29}H_{24}Fe_2SCl_2$, triclinic, space group $P\bar{1}$ (#2), $a = 10.429(2)$ Å, $b = 11.043(2)$ Å, $c = 11.191(2)$ Å, $\alpha = 83.94(2)°$, $\beta = 68.99(2)°$, $\gamma = 84.01(2)°$, $V = 1193.4(5)$ Å^3, $Z = 2$, $D_{calcd} = 1.634$ g cm^{-3}, $T = 123 \pm 1$ K, $\lambda(MoK_\alpha) = 0.71075$ Å. 10,031 reflections measured, 4830 unique ($R_{int} = 0.045$). The final cycle of full-matrix least-squares refinement was based on 4405 observed reflections ($I > 2.00\sigma(I)$) and 403 variable parameters with $R_1 = 0.046$, $wR_2 = 0.112$ (all data) (CCDC 299170).
13. Crystal data for **2**: $M = 502.24$, $C_{28}H_{22}Fe_2S$, monoclinic, space group $P2_1/c$ (#14), $a = 11.9107(8)$ Å, $b = 14.1854(8)$ Å, $c = 12.218(1)$ Å, $\beta = 92.359(3)°$, $V = 2062.6(3)$ Å^3, $Z = 4$, $D_{calcd} = 1.617$ g cm^{-3}, $T = 123 \pm 1$ K, $\lambda(MoK_\alpha) = 0.71075$ Å. 20,093 reflections measured, 4721 unique ($R_{int} = 0.033$). The final cycle of full-matrix least-squares refinement was based on 4721 observed reflections ($I > 2.00\sigma(I)$) and 368 variable parameters with $R_1 = 0.025$, $wR_2 = 0.031$ (all data) (CCDC 299169).
14. Crystal data for **3**: $M = 549.14$, $C_{28}H_{22}Fe_2Se$, monoclinic, space group $P2_1/a$ (#14), $a = 12.139(4)$ Å, $b = 14.190(5)$ Å, $c = 12.083(4)$ Å, $\beta = 92.01(2)°$, $V = 2080(1)$ Å^3, $Z = 4$, $D_{calcd} = 1.753$ g cm^{-3}, $T = 123 \pm 1$ K, $\lambda(MoK_\alpha) = 0.71075$ Å. 19,106 reflections measured, 4593 unique ($R_{int} = 0.089$). The final cycle of full-matrix least-squares refinement was based on 3783 observed reflections ($I > 2.00\sigma(I)$) and 368 variable parameters with $R_1 = 0.041$, $wR_2 = 0.114$ (all data) (CCDC 299168).
15. Bryan, C. D.; Cordes, A. W.; Haddon, R. C.; Hicks, R. G.; Oakley, R. T.; Palstra, T. T. M.; Perel, A. J. *J. Chem. Soc., Chem. Commun.* **1994**, 1447–1448.